

Pressure-induced change in the electronic structure of epitaxially strained $\text{La}_{1-x}\text{Sr}_x\text{MnO}_3$ thin films

K. Horiba,^{1,2,3,*} A. Maniwa,¹ A. Chikamatsu,¹ K. Yoshimatsu,¹ H. Kumigashira,^{1,2,3} H. Wadati,⁴ A. Fujimori,⁴ S. Ueda,⁵ H. Yoshikawa,⁵ E. Ikenaga,⁶ J. J. Kim,⁶ K. Kobayashi,^{5,6} and M. Oshima^{1,2,3}

¹Department of Applied Chemistry, The University of Tokyo, Tokyo 113-8656, Japan

²Synchrotron Radiation Research Organization, The University of Tokyo, Tokyo 113-8656, Japan

³Core Research for Evolutional Science and Technology (CREST), Japan Science and Technology Agency, Tokyo 102-0075, Japan

⁴Department of Physics, The University of Tokyo, Tokyo 113-0033, Japan

⁵NIMS/SPRING-8, Hyogo 679-5148, Japan

⁶JASRI/SPRING-8, Hyogo 679-5198, Japan

(Received 15 September 2009; published 21 October 2009)

We report the observation of pressure-induced changes in the electronic structures of $\text{La}_{1-x}\text{Sr}_x\text{MnO}_3$ (LSMO) by hard x-ray photoemission spectroscopy. Application of compressive and tensile strains results in the formation of a gap at the Fermi level (E_F) and suppression of spectral weight at E_F , respectively, across magnetic phase transitions. In contrast, no detectable change is observed in the absence of phase transitions even upon application of pressure. These results indicate that the change in the electronic structure of LSMO does not originate from the lattice distortions alone, but is induced by subtle interplay among the lattice, magnetic, and orbital degrees of freedom.

DOI: [10.1103/PhysRevB.80.132406](https://doi.org/10.1103/PhysRevB.80.132406)

PACS number(s): 75.47.Gk, 71.30.+h, 79.60.-i, 78.20.Bh

Pressure is one of the most crucial parameters for controlling the physical properties of solids. It specifically changes the bandwidth without causing any chemical fluctuations or disorders concomitant with chemical substitution, i.e., chemical pressure. The effects of pressure on the properties of strongly correlated electron systems (SCESs) are drastic since the unique physical properties of these systems arise from strong mutual coupling among the spin, charge, orbital, and lattice degrees of freedom.^{1,2} Therefore, the effects of pressure on the physical properties of SCESs have been extensively investigated by using transport measurements and various spectroscopic methods.

Photoemission spectroscopy (PES) is a unique and powerful experimental technique that enables the direct determination of density of states (DOS) in condensed matter. However, the observation of the electronic structure under physical hydrostatic pressure is very difficult using this technique. This is because photoelectrons cannot be picked up from inside of a high-pressure cell owing to a fundamental limitation of this technique. Therefore, the application of PES has been limited to the study of the changes in the electronic structure associated with chemical substitutions. However, if SCESs are epitaxially grown on single-crystalline substrates in the form of a thin film,³⁻⁵ it will be possible to effectively perform photoemission measurements under (anisotropic) high pressure. The effect of anisotropic pressure on such SCESs should be remarkable particularly with respect to charge-orbital-related phenomena because the charge and orbital degrees of freedom are strongly coupled with lattice distortion.

A particularly promising aspect of such SCESs is the orbital-state-mediated phase control of manganites using the epitaxial lattice strain from substrates.^{3,5,6} Konishi *et al.*³ reported that the physical properties of $\text{La}_{1-x}\text{Sr}_x\text{MnO}_3$ (LSMO) thin films are sensitive to tetragonal distortion, and they deduced a phase diagram of hole doping (x) vs lattice-constant

ratio (c/a), which is the ratio of the out-of-plane lattice constant to the in-plane lattice constant, as shown in Fig. 1(a). LSMO bulk crystals with $x=0.4$ and $x=0.5$ exhibit ferromagnetic metallic (FM) properties. These properties of LSMO can be explained on the basis of a double-exchange mechanism as follows.² In the regular octahedron of MnO_6 of the perovskite LSMO, Mn $3d$ orbitals split into doubly degenerate e_g and triply degenerate t_{2g} orbitals because of crystal-field splitting. Holes doped into the Mn $3d$ e_g orbitals act as mobile charge carriers and undergo strong Hund's coupling with the localized Mn $3d$ t_{2g} spins, resulting in the stabilization of ferromagnetism in LSMO. The properties of LSMO thin films with $x=0.4$ and $x=0.5$ grown on $(\text{LaAlO}_3)_{0.3}-(\text{SrAl}_{0.5}\text{Ta}_{0.5}\text{O}_3)_{0.7}$ (LSAT) substrates are almost the same as those of the LSMO bulk crystals because the lattice constants of LSMO and LSAT (3.870 Å) are approximately the same. When LSMO thin films are grown on LaAlO_3 (LAO) substrates, which have a smaller lattice con-

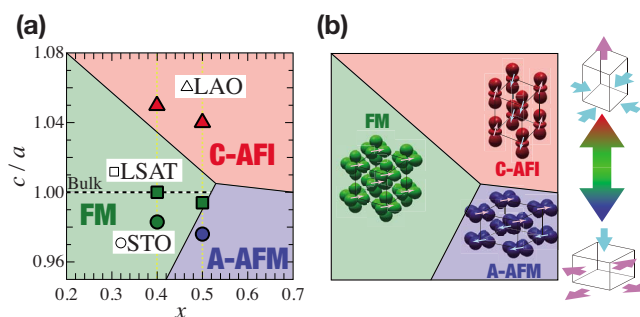


FIG. 1. (Color online) (a) Phase diagram of LSMO films in the plane of lattice-constant ratio (c/a) and doping level (x) (Ref. 3). The triangles, squares, and circles indicate the HX-PES measurement points of LSMO thin films grown on LAO, LSAT, and STO substrates, respectively. (b) Schematic illustrations of spin and orbital configurations in C-AFI, FM, and A-AFM phases.

stant (3.792 Å) than LSMO, the LSMO thin films experience compressive strain in the ab plane causing the c axis to elongate. Therefore, the value of c/a becomes 1.05, which corresponds to a biaxial pressure of ~ 10 GPa. This distortion stabilizes the $d_{3z^2-r^2}$ orbital, and LSMO/LAO films exhibit C-type antiferromagnetic ordering with insulating properties (C-AFI). On the other hand, when LSMO thin films are grown on SrTiO₃ (STO) substrates, which have a larger lattice constant (3.905 Å) than LSMO, the LSMO thin films experience tensile strain in the ab plane, and the c axis is compressed. Because of this physical pressure, LSMO thin films with $x=0.5$ grown on STO substrates exhibit A-type antiferromagnetic metallic (A-AFM) properties with $d_{x^2-y^2}$ orbital ordering. The spin and orbital configurations of the LSMO thin films in each phase are illustrated in Fig. 1(b).

This method of applying physical pressure on a crystal system without the use of a high-pressure cell enables the direct observation of the electronic structure under physical pressure.^{7–10} In this Brief Report, we report the observation of changes in the electronic structures of LSMO thin films induced by physical pressure using hard x-ray PES (HX-PES).^{11,12} We found that the application of compressive ($c/a=1.05$) and tensile ($c/a=0.98$) strain results in the formation of a gap at the Fermi level (E_F) and suppression of spectral weight at E_F , respectively, across the phase transitions. By comparing the present HX-PES results with the physical properties and band-structure calculations, we discuss the physical nature of the orbital-state-mediated phase transitions of manganites.

LSMO thin films were epitaxially grown on atomically flat surfaces of LAO, LSAT, and Nb-doped STO substrates by using laser molecular-beam epitaxy.^{13,14} LSMO thin films were deposited on the LSAT and STO substrates at a substrate temperature of 1050 °C and on the LAO substrates at a substrate temperature of 400 °C, under oxygen pressure of 1×10^{-4} Torr. The thickness of the films was accurately determined by reflection high-energy electron-diffraction intensity oscillations; it was found to be 100 monolayers (≈ 400 Å). The LSMO thin films were subsequently annealed at 400 °C for 45 min in atmospheric pressure of oxygen in order to remove oxygen vacancies. The crystal structure of the prepared thin films was characterized by four-circle x-ray diffraction measurements. We confirmed that the in-plane lattice constants of all LSMO films match with those of the substrates. The electrical resistivity was measured by the four-probe method. Magnetization was measured by using a superconducting quantum interference device magnetometer with the magnetic field applied along the [100] axis parallel to the surface. We confirmed that all the films exhibit the same electrical and magnetic properties as those reported in the previous studies.^{3,6}

HX-PES experiments were carried out at undulator beamlines BL15XU and BL47XU of SPring-8. X-rays were monochromatized at 5.95 keV by using a Si(111) double-crystal monochromator. A channel-cut monochromator with Si(333) reflection placed downstream of the double-crystal monochromator reduced the energy bandwidth to 50 meV. The total energy-resolution was set to 250 meV for core-level and valence-band measurements and 150 meV for high-resolution measurements near E_F . The energy position was

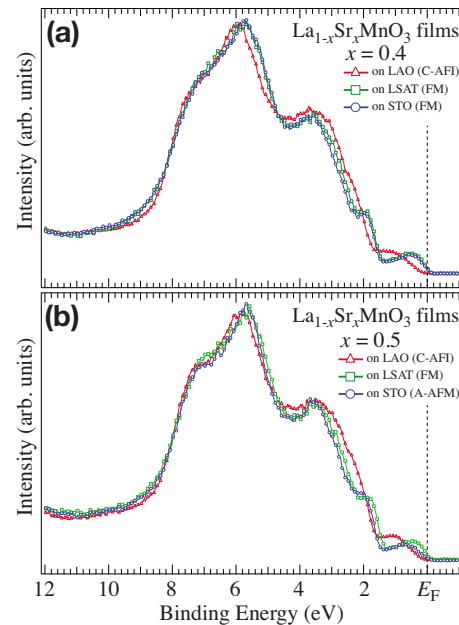


FIG. 2. (Color online) Valence-band HX-PES spectra of LSMO thin films with (a) $x=0.4$ and (b) $x=0.5$, grown on LAO, LSAT, and STO substrates.

calibrated by measuring the Fermi-edge profile of a gold plate. The PES spectra of LSMO films grown on LSAT substrates (LSMO/LSAT) and LSMO films grown on STO substrates (LSMO/STO) were measured at 40 K, while the PES spectra of LSMO films grown on LAO substrates (LSMO/LAO) were measured at 120 K to avoid the charging effect. We confirmed that the spectra of LSMO/LSAT and LSMO/STO measured at 40 K were not significantly different from their corresponding spectra measured at 120 K.

Figure 2 shows the valence-band HX-PES spectra of LSMO thin films with different doping levels and under different strain effects. The overall line shapes of the valence-band spectra of all LSMO films are almost the same. Clear peak structures observed around 6 eV, 3.5 eV, 2 eV, and near E_F are assigned to O $2p$ bonding states, O $2p$ nonbonding states, Mn $3d t_{2g}$ states, and Mn $3d e_g$ states, respectively.¹⁴ The O $2p$ bonding states in the spectra of LSMO/LAO slightly shift to a higher binding energy than those in other films. Simultaneously, it is observed at around 8 eV, the high-binding-energy tail of these O $2p$ bonding states decreases, indicating the narrowing of the O $2p$ band. These spectroscopic behaviors are commonly observed in HX-PES spectra across metal-insulator transitions of other transition-metal oxides.¹⁵ Therefore, it is suggested that the spectral changes observed in the case of LSMO/LAO are attributed to the antiferromagnetic insulating properties of these films.

In contrast to the O $2p$ states, Mn $3d$ states near E_F exhibit significant changes. In order to investigate the spectral changes in the Mn $3d$ states, which are directly coupled with the physical properties of LSMO, in further detail, we measured the HX-PES spectra near E_F with higher energy resolution. The resultant spectra are shown in Fig. 3. In the spectra of both LSMO films with $x=0.4$ and $x=0.5$, the electronic structures of LSMO/LAO are significantly different from

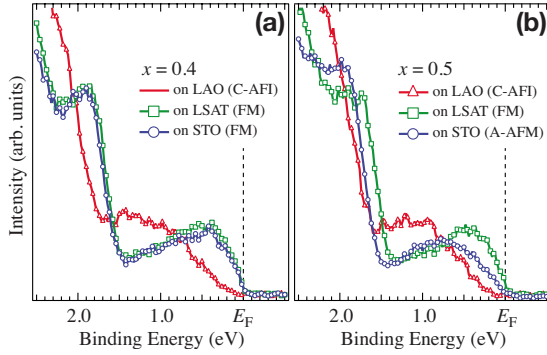


FIG. 3. (Color online) High-resolution HX-PES spectra near E_F of LSMO thin films with (a) $x=0.4$ and (b) $x=0.5$, grown on LAO, LSAT, and STO substrates.

those of other films. The Mn $3d e_g$ states near E_F shift to a higher binding energy, and energy gaps are formed at E_F , indicating the insulating properties of LSMO/LAO in the C-AFI phase. Concurrently, it is observed that the t_{2g} states around 2 eV of LSMO/LAO shift slightly to a higher binding energy than those of LSMO/LSAT and LSMO/STO. A similar shift in the t_{2g} states to a higher binding energy, accompanied by the destabilization of ferromagnetic states, has been reported in studies on $\text{Nd}_{1-x}\text{Sr}_x\text{MnO}_3$ bulk crystals¹⁶ and temperature dependence of ferromagnetic LSMO thin films.¹⁷

When we compare the spectra among the metallic LSMO/LSAT and LSMO/STO, the suppression of DOS near E_F and the shift in both Mn $3d e_g$ and t_{2g} states to a higher binding energy, are observed only in the spectrum of LSMO/STO with $x=0.5$. The suppression of spectral weight at E_F has also been reported in optical conductivity measurements,⁶ suggesting that the metallic DOS at E_F is suppressed by the antiferromagnetic fluctuations in LSMO/STO with $x=0.5$. On the other hand, in the case of LSMO films with $x=0.4$, the spectrum of LSMO/STO is almost identical to that of LSMO/LSAT.

The change in the electronic structure of the films is further supported by the Mn $2p$ core-level HX-PES spectra shown in Fig. 4. The appearance of a sharp peak at the low-binding-energy side of the Mn $2p_{3/2}$ main peak has been interpreted as a well-screened feature arising from metallic DOS at E_F ; this is known to be closely related to the FM phase of LSMO thin films.^{10,18} The intensity of this peak in

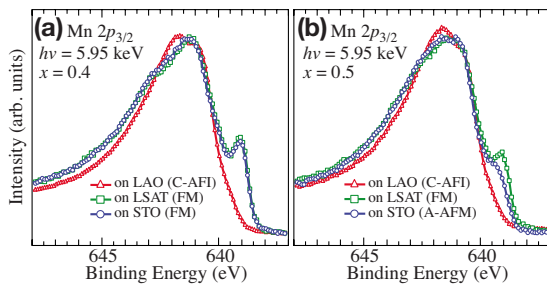


FIG. 4. (Color online) Mn $2p_{3/2}$ core-level HX-PES spectra of LSMO thin films with (a) $x=0.4$ and (b) $x=0.5$, grown on LAO, LSAT, and STO substrates.

the spectra of LSMO/LSAT and LSMO/STO with $x=0.4$ is almost the same. In contrast, this sharp peak disappears in the spectrum of LSMO/LAO with $x=0.4$, corresponding to the occurrence of a pressure-induced metal-insulator transition. Similarly, in the spectra of LSMO films with $x=0.5$, the peak attributable to the well-screened feature is observed in the spectrum of LSMO/LSAT (FM phase), and it disappears in the spectrum of LSMO/LAO (C-AFI phase), as shown in Fig. 4(b). The significant difference between the spectra of the films with $x=0.4$ and $x=0.5$ is the decrease in the intensity of the peak in the spectrum of LSMO/STO with $x=0.5$. This decrease is consistent with the suppression of the metallic DOS at E_F observed in the valence-band spectra of these films.¹⁹

The observed spectral changes are more typical of the transport and magnetic properties than of the degree of lattice distortions. In the case of LSMO films with $x=0.5$, LSMO/LSAT that are almost free from strain exhibit FM properties, while LSMO/STO with a c/a ratio of 0.98 exhibit A-AFM properties. However, in the case of LSMO films with $x=0.4$, both LSMO/LSAT and LSMO/STO show FM properties irrespective of strain; the c/a ratio in LSMO/STO becomes 0.98 on the application of tensile strain, while LSMO/LSAT do not experience strain. If the electronic structure of LSMO was a direct consequence of the lattice distortions alone, then the changes observed in the spectra of LSMO/STO with $x=0.4$ would be similar to those observed in the spectra of LSMO/STO with $x=0.5$, since both the films experience a large amount of tensile strain. Therefore, this consistency between the spectral observations of LSMO/LSAT and those of LSMO/STO with $x=0.4$ indicates that lattice distortions alone do not considerably affect the electronic structure of LSMO films. Thus, the magnetic and orbital ordering simultaneously induced by the biaxial strain play a dominant role in changing the electronic structure of LSMO films. Since the changes in the electronic structure are not induced by the lattice distortions, but by the quantum fluctuations of the magnetic nature, one can consider the phase transitions occurring in epitaxially strained LSMO thin films as suitable examples of quantum phase transitions induced by physical pressure.

On the basis of band-structure calculations, Fang *et al.*²⁰ have demonstrated that orbital ordering is related to not only the lattice distortion but also magnetic ordering. Under the same amount of strain, antiferromagnetic ordering occurs more easily in LSMO with $x=0.5$ than in LSMO with $x=0.4$, because the double-exchange interaction becomes weak as a result of the reduction in e_g spins on hole doping. In the calculated DOS, degenerated e_g orbitals in the FM phase are split into $d_{x^2-y^2}$ and $d_{3z^2-r^2}$ orbitals in the A-type antiferromagnetic (A-AF) or C-type antiferromagnetic (C-AF) phase. This splitting causes the centroid of Mn $3d e_g$ states in the A-AF and C-AF phases to shift to a higher binding energy. This shift is consistent with the experimental spectral observations. The calculations suggest that the contribution of magnetic ordering to splitting of e_g orbitals is more than that of crystal-field splitting caused by tetragonal distortions. However, the calculations fail to reproduce the energy gap at E_F that is clearly observed in HX-PES spectra of LSMO films in C-AFI phase. Furthermore, the significant

suppression of the DOS at E_F observed in the HX-PES spectra even in the FM phase cannot be explained by the band calculations, suggesting the importance of many-body effects such as strong electron-electron interactions and electron-phonon coupling.

In conclusion, we have performed HX-PES measurements on LSMO thin films across phase transitions under the physical pressure induced by the epitaxial strain from the substrates. In the HX-PES spectra, we observed the suppression of DOS at E_F for the A-AFM phase in LSMO/STO with $x=0.5$ and the gap formation at E_F for the C-AFI phase in LSMO/LAO. The difference between the electronic structures of LSMO/STO with $x=0.4$ and those of LSMO/STO with $x=0.5$ indicates that the magnetic and orbital ordering

induced by the tetragonal lattice distortion plays a dominant role in changing the electronic structure of strained LSMO thin films. Thus, we have demonstrated the capability of PES under physical pressure by using epitaxial strain for investigating the correlation among lattice distortions, magnetic ordering, and orbital ordering of SCESs.

The authors would like to thank staff in HiSOR of Hiroshima University and JAEA/SPring-8 for the developing HX-PES at BL15XU of SPring-8. The authors would also like to thank D. D. Sarma for his helpful discussions. This work was supported by a Grant-in-Aid for Scientific Research (Grants No. A19684010 and No. B19740199) from JSPS.

*horiba@sr.t.u-tokyo.ac.jp

- ¹M. Imada, A. Fujimori, and Y. Tokura, *Rev. Mod. Phys.* **70**, 1039 (1998).
- ²Y. Tokura in *Colossal Magnetoresistive Oxides*, Advances in Condensed Matter Science Vol. 2 (Gordon and Breach, Amsterdam, 2000).
- ³Y. Konishi, Z. Fang, M. Izumi, T. Manako, M. Kasai, H. Kuwahara, M. Kawasaki, K. Terakura, and Y. Tokura, *J. Phys. Soc. Jpn.* **68**, 3790 (1999).
- ⁴A. D. Rata, A. Herklotz, K. Nenkov, L. Schultz, and K. Dörr, *Phys. Rev. Lett.* **100**, 076401 (2008).
- ⁵Y. Takamura, R. V. Chopdekar, E. Arenholz, and Y. Suzuki, *Appl. Phys. Lett.* **92**, 162504 (2008).
- ⁶Y. Okimoto, Y. Konishi, M. Izumi, T. Manako, M. Kawasaki, and Y. Tokura, *J. Phys. Soc. Jpn.* **71**, 613 (2002).
- ⁷M. Abrecht, D. Ariosa, D. Cloetta, S. Mitrovic, M. Onellion, X. X. Xi, G. Margaritondo, and D. Pavuna, *Phys. Rev. Lett.* **91**, 057002 (2003).
- ⁸D. Cloetta, D. Ariosa, C. Cancellieri, M. Abrecht, S. Mitrovic, and D. Pavuna, *Phys. Rev. B* **74**, 014519 (2006).
- ⁹H. Wadati, A. Maniwa, A. Chikamatsu, I. Ohkubo, H. Kumigashira, M. Oshima, A. Fujimori, M. Lippmaa, M. Kawasaki, and H. Koinuma, *Phys. Rev. Lett.* **100**, 026402 (2008).
- ¹⁰H. Tanaka, Y. Takata, K. Horiba, M. Taguchi, A. Chainani, S. Shin, D. Miwa, K. Tamasaku, Y. Nishino, T. Ishikawa, E. Ikenaga, M. Awaji, A. Takeuchi, T. Kawai, and K. Kobayashi, *Phys. Rev. B* **73**, 094403 (2006).
- ¹¹K. Kobayashi, M. Yabashi, Y. Takata, T. Tokushima, S. Shin, K. Tamasaku, D. Miwa, T. Ishikawa, H. Nohira, T. Hattori, Y. Sugita, O. Nakatsuka, A. Sakai, and S. Zaima, *Appl. Phys. Lett.* **83**, 1005 (2003).
- ¹²Y. Takata, in *Very High Resolution Spectroscopy*, edited by S. Hüfner (Springer, New York, 2007), Chap. 14.
- ¹³K. Horiba, H. Ohguchi, H. Kumigashira, M. Oshima, K. Ono, N. Nakagawa, M. Lippmaa, M. Kawasaki, and H. Koinuma, *Rev. Sci. Instrum.* **74**, 3406 (2003).
- ¹⁴K. Horiba, A. Chikamatsu, H. Kumigashira, M. Oshima, N. Nakagawa, M. Lippmaa, K. Ono, M. Kawasaki, and H. Koinuma, *Phys. Rev. B* **71**, 155420 (2005).
- ¹⁵R. Eguchi, M. Taguchi, M. Matsunami, K. Horiba, K. Yamamoto, Y. Ishida, A. Chainani, Y. Takata, M. Yabashi, D. Miwa, Y. Nishino, K. Tamasaku, T. Ishikawa, Y. Senba, H. Ohashi, Y. Muraoka, Z. Hiroi, and S. Shin, *Phys. Rev. B* **78**, 075115 (2008).
- ¹⁶A. Sekiyama, H. Fujiwara, A. Higashiya, S. Imada, H. Kuwahara, Y. Tokura, and S. Suga, arXiv:cond-mat/0401601 (unpublished).
- ¹⁷K. Horiba, A. Chikamatsu, H. Kumigashira, M. Oshima, H. Wadati, A. Fujimori, M. Lippmaa, M. Kawasaki, and H. Koinuma, *J. Electron Spectrosc. Relat. Phenom.* **156-158**, 375 (2007).
- ¹⁸K. Horiba, M. Taguchi, A. Chainani, Y. Takata, E. Ikenaga, D. Miwa, Y. Nishino, K. Tamasaku, M. Awaji, A. Takeuchi, M. Yabashi, H. Namatame, M. Taniguchi, H. Kumigashira, M. Oshima, M. Lippmaa, M. Kawasaki, H. Koinuma, K. Kobayashi, T. Ishikawa, and S. Shin, *Phys. Rev. Lett.* **93**, 236401 (2004).
- ¹⁹Note that the well-screened peak in the spectra of LSMO/LSAT with $x=0.5$ seems to be smaller than that in the spectra of LSMO/LSAT with $x=0.4$ because the well-screened feature is derived from Mn^{3+} ($3d^5\bar{C}$ configuration), and contribution of Mn^{4+} to the intensity of the Mn $2p$ main peak in LSMO films $x=0.5$ is larger than that in LSMO films with $x=0.4$.
- ²⁰Z. Fang, I. V. Solovyev, and K. Terakura, *Phys. Rev. Lett.* **84**, 3169 (2000).